LUND UNIVERSITY

Experimental evaluation of MIMO terminal antenna configurations in noise- and interference-limited urban scenarios

Plicanic, Vanja; Lau, Buon Kiong; Asplund, Henrik

Link to publication

V. Plicanic, B. K. Lau, and H. Asplund, "Experimental evaluation of MIMO terminal antenna configurations in noise- and interference-limited urban scenarios," in *Proc. 5th Europ. Conf, Antennas Propagat. (EuCAP'2011)*, Rome, Italy, Apr. 11-15, 2011.

Experimental evaluation of MIMO terminal antenna configurations in noise- and interference-limited urban scenarios

Vanja Plicanic[#+], Buon Kiong Lau[+], Henrik Asplund[*]

[#] *Sony Ericsson Mobile Communication AB*
SE-221 00 Lund, Sweden
vanja.plicanic@sonyericsson.com
[+] *Department of Electrical and Information Technology, Lund University*
SE-221 00 Lund, Sweden
{vpc,bkl}@eit.lth.se
[*] *Ericsson AB*
SE-164 83 Kista, Sweden
henrik.asplund@ericsson.com

Abstract—In this paper, we compare capacity performances of three terminal dual-antenna configurations at 2.65 GHz based on extensive 2 by 2 multiple-input multiple-output (MIMO) channel measurements in an urban macrocellular environment. Both noise- and interference-limited scenarios are investigated. Our results show that, on average over the measurement route, the capacity performance is mainly determined by the received power. However, locally along the route, the eigenvalue dispersion of the channel can be the dominant factor that influences the capacity performance. In addition, significant differences in the local performances of the terminal antenna configurations along the route give an indication that antenna reconfigurability is a promising approach to maximize capacity.

I. INTRODUCTION

Due to recent, although still limited, deployment of the Long Term Evolution (LTE) for mobile communications, the smart phone industry is urgently addressing the challenges of implementing multiple co-band antennas in compact devices. Practical performance investigations and analyses of multiple antenna configurations for multiple-input multiple-output (MIMO) purposes have been performed in indoor and outdoor scenarios in [1]-[3]. However, the focus has been on the comparison between mobile devices of different forms and sizes, such as laptops, mobile phones and data cards. Moreover, one main conclusion is that, on average, different antenna configurations have similar capacity performances, as long as the antenna efficiencies are similar [2], [3].

This study focuses on the capacity performances of three simple dual-antenna topologies that are based on the available space for antenna implementation in a realistic, typical size, smart phone prototype. The purpose is to determine the potential of antenna system design as one key performance differentiator among different terminals. Thus, the capacity performances were obtained through an extensive 2 × 2 MIMO channel measurement campaign at 2.65 GHz in an urban propagation environment. Moreover, the evaluations are performed for noise-limited (NL) and interference-limited (IL) scenarios to further tie the contribution to realistic cases.

The measurement campaign is described in Section II. In Section III, the terminal and reference antenna configurations are presented. This is followed by results and discussions in Section IV. In Section V, the conclusions are provided.

II. MIMO CHANNEL MEASUREMENTS

The MIMO channel measurements were conducted with a non-commercial wideband channel sounder operating at 2.65 GHz. Three pairs of the eight transmit (TX) branches were utilized for this study. They were connected to three dual-polarized, sector-covering antennas on a roof-top base station (BS), which was at height of 23 m above ground level. The TX antenna configurations enable a three-sector site similar to those commonly deployed in wireless cellular systems. One receive (RX) dual-antenna prototype at a time was connected to the receiver. The prototype is vertically-oriented and attached to an electrically neutral fixture on the roof of a van (i.e., free space (FS) case) used as a mobile station (MS).

The measurement campaign was conducted in an urban macrocellular environment in the northern part of Stockholm, Sweden. A snapshot of the 20 MHz MIMO channel was recorded every 5.33 ms over a predefined 2 km drive route within the three-sector site. The driving was conducted with speed not exceeding 30 km/h to ensure Nyquist sampling of at least two measurement points per traveled wavelength (λ). GPS positioning was used to simplify the comparison of consecutive measurements with different antenna configurations. A 600 m section of the route (see Fig. 1) is chosen to demonstrate representative results of the entire route.

III. TERMINAL AND REFERENCE ANTENNA CONFIGURATIONS

Three antenna configurations at 2.65 MHz are investigated in this contribution. They represent different cases of practical, dual-antenna placement in terminal-like prototypes. Each configuration comprises two single band antennas on the

ground plane of size 111×61 mm^2 in a prototype of size $118 \times 65 \times 11$ mm^3 (see Fig. 2). The configurations are chosen to reflect spatial and closely-located implementations of multiple antennas. Configuration A represents the spatial case. The top and bottom placed antennas in prototype A are simple folded monopoles with a feed separation of 95 mm (i.e., 0.8λ at 2.65 GHz). Prototypes B and C comprise closely spaced and orthogonally placed notch antennas with feed separations of 11 mm and 6 mm (i.e., less than 0.1λ at 2.65 GHz), respectively. In this study, the antenna volume and placement were designed around a 3.5 inch display to account for some typical implementation constraints in terminal prototypes.

Two reference configurations, (1) spatial and (2) cross polarization, were also evaluated in this study. The antennas in the spatial reference are vertically-oriented half-wavelength dipoles separated by 0.5λ. In the cross polarization configuration, the two antennas (vertical and horizontal half-wavelength dipoles) are separated by 0.25λ. The reference configurations represent close to ideal cases of dual-antenna design for exploiting the (1) spatial and (2) polarization (and angular) properties of the channel at the MS side.

The total antenna efficiencies and the correlation of the terminal and reference configurations in uniform 3D angular power spectrum (APS) are presented in Table I. The radiation and polarization behaviors of the two antennas in each of the three terminal configurations are presented in Fig. 3(a)-(f). The figures show different angular coverage enabled by each of the antennas in each of the terminal prototypes, as well as different polarization states at these radiation angles. Thus, all three configurations exploit angle and polarization diversity. Furthermore, spatial diversity is exploited in prototype A due to its relatively large antenna separation.

IV. MIMO PERFORMANCE ANALYSIS AND DISCUSSIONS

Average channel gain, eigenvalue dispersion (ED) of the channel expressed in the form of ellipticity statistic (ES) [4], [5] and MIMO channel capacity for both NL [6] and IL [7] scenarios are evaluated for 2×2 TX-RX configurations. At each point (or MS location) along the route, the channel gains of the three BS sectors are compared. The sector with the highest gain is chosen to be representative of that specific point. Hence, all the figure-of-merits in this paper are based on switching among the BS sectors along the drive route. MIMO capacity is evaluated at each point along the route at the corresponding signal-to-noise ratio (SNR) which, for *all* mentioned configurations, is in a range of 15-40 dB. All the calculations are based on data with fast fading averaged out over ten wavelengths (1.1 m) along the route.

A. Noise-Limited (NL) Scenario

The capacity performances of TX-RX configurations with the three terminal antenna configurations at RX are presented in Fig. 4. For most part of the route, the performances between the cases are similar. However, there are obvious differences in some sections of the route. To understand these differences, the average local capacities of the three terminal prototypes are
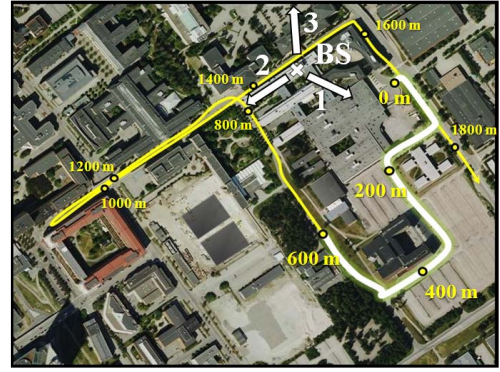

Fig. 1 Drive route in the measurement campaign. The thick line marks the 600 m route under investigation. The arrows at the BS indicate the main beam directions of the TX antenna configurations (Sectors 1, 2 and 3).
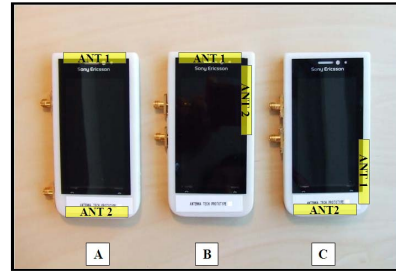

Fig. 2 Locations of the antennas for each of the three terminal prototypes.

TABLE I
TOTAL ANTENNA EFFICIENCIES AND ENVELOPE CORRELATION OF THE DUAL-ANTENNA CONFIGURATIONS IN FREE SPACE

Antenna configurations	Total antenna efficiency [dB]		Envelope correlation
	ANT 1	ANT 2	
A	-2.8	-2.1	0.1
B	-2.3	-4.1	0.1
C	-3.9	-1.9	0.1
Spatial reference	-1.6	-1.5	0.1
Cross pol. reference	-1.2	-1.4	0.1

obtained for three representative 10 m sections of the route (with center points at 260 m, 430 m and 460 m). The sections are chosen such that the propagation characteristics within each section are fairly consistent. The maximum difference in average capacity (or peak improvement) among the prototypes for three shorter 1.1 m sections (i.e., the removal of fast fading) with the same three center points are also taken from Fig. 4.

The average local capacities for the NL scenario are shown in Table II. At 260 m, prototype B enables 16% higher average capacity than prototype C for the 10 m section. The peak improvement is 18%. Here, the propagation environment is line-of-sight (LOS), with the LOS angle-of-arrival (AoA) of $\phi \sim$ -80°. Rician K-factors of up to 14.6 dB and 3.2 dB are observed for the channel coefficients in the cases of prototypes B and C, respectively. Hence, the channel gain of B is higher than that of C by $\sim$4 dB, as seen in Fig. 5. Furthermore, prototype B has low ED (i.e., ES $\sim$0.76 at the center point of the section, see Fig. 6), which is enabled by polarization diversity. This means that the antennas in prototype B, as compared to the other two prototypes, have
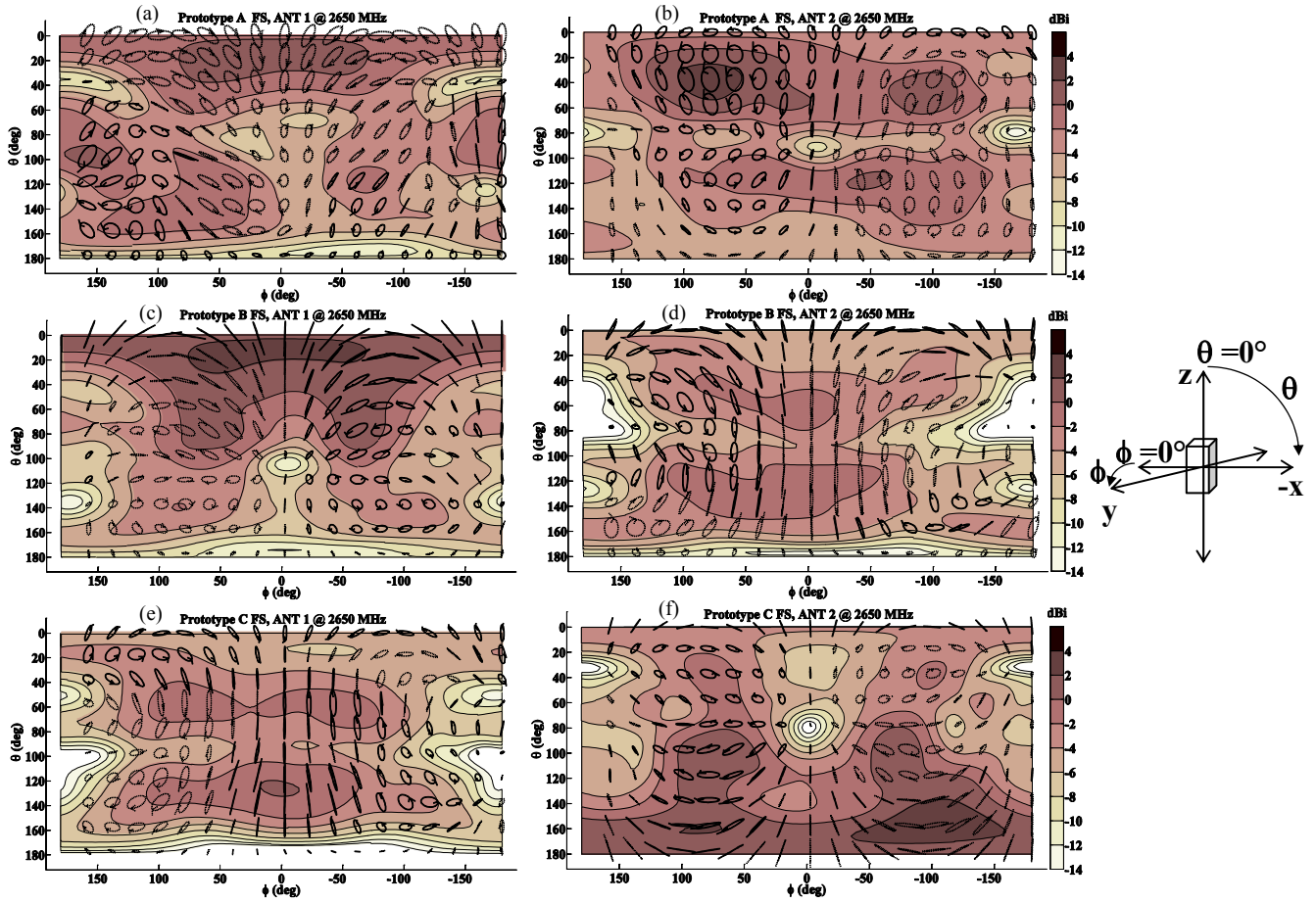
Fig. 3 2D presentation of 3D realized gain and polarization states (dotted line circles = right hand circular polarization, solid line circles = left hand circular polarization) of the two antenna ports for each of the three prototypes A (a)-(b), B (c)-(d) and C (e)-(f) at 2.65 GHz and FS scenario. In the measurements, the terminals were placed vertically in the coordinate system, as shown above, with the terminal's back side facing the direction of movement along the y-axis.

the best angular and polarization alignment with the LOS signal, thus assuring that B has the best capacity performance.

Prototype C collects the least power despite its low ED (ES ~0.72 at the center point of the section). The low K-factor and ED indicate that prototype C collects the power mainly through multipaths. The angular patterns of the antennas in prototype C, in contrast to those of prototypes A and B, are oriented towards larger elevation angles, i.e., mainly towards the ground (see Fig. 3(a)-(f)). Since the AoA of the LOS path is at a smaller elevation angle, there is less alignment between the angular patterns and the dominant path. Prototype A has higher ED (ES ~0.45 at the center point of the section) and a K-factor of 9 dB. This suggests that good alignment between the antenna patterns and the dominant path ensures that A has a 3 dB better channel gain than C. Nevertheless, prototype C has comparable capacity performance to that of A, since its better ED performance compensates for its lower channel gain.

At the 10 m section at 430 m (i.e., non-LOS), prototype A enables the best average capacity, which is approximately 9% higher than those of B and C. The peak capacity improvement, found at the center point of the section, is 15%. Prototype C has similar channel gain performance to that of A. Nevertheless, the capacity of C is lower due to its high ED (ES ~0.29). Thus, the lack of multipath richness and/or

polarization diversity is the reason behind the low capacity performance. Assuming that ED variation can be seen as SNR variation as suggested in [4], [8] for Rayleigh cases and high SNRs, prototype A has a 10 $\log_{10}(0.75/0.29)$ = 4.1 dB advantage by means of ED over prototype C, at the center point of the section. Prototype B further highlights the importance of ED since, despite its 2.2 dB lower channel gain, it has similar capacity as C. Here, the low channel gain is compensated by a 10 $\log_{10}(0.53/0.29)$ = 2.6 dB gain in ED.

At 460 m, the 10 m section is also characterized by NLOS propagation, but the best average performance is enabled by prototype B. Prototype B has 12% higher capacity than prototype C, which has the lowest capacity among the three prototypes. The peak improvement is 16%. Here, prototype B has advantage not only in channel gain, since it collects 2 dB more power than prototype C, but also by means of lower ED (ES ~0.80) as compared to the ED (ES ~0.5) of prototype C. Hence, the 10 $\log_{10}(0.8/0.5)$ = 2 dB advantage in ED and the 2 + 2 = 4 dB net advantage enables the peak improvement.

The cumulative distribution functions (CDFs) of capacity performances for the three prototypes over the 600 m route are shown in Fig. 7. Low ED and similar channel gains for the three prototypes result in very similar 50% outage capacities. However, the performances of the two reference antennas are
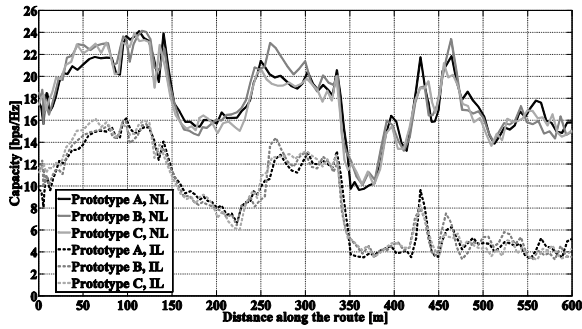
Fig. 4 Average capacity in the NL and IL scenarios for different TX–RX configurations.
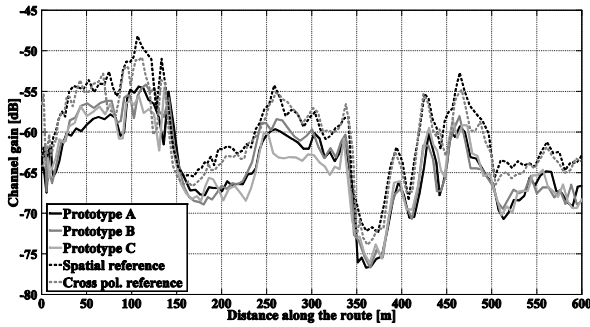

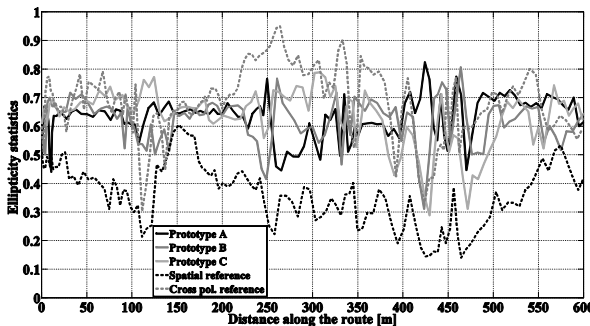Fig. 5 Average channel gains per receive antenna and 20 MHz bandwidth for different TX–RX configurations.

Fig. 6 Ellipticity statistic (ES) for different TX-RX configurations.

different. Since the channel gains for the reference configurations are similar along the route (see Fig. 5), the ED performances are decisive of the capacity performances. Thus, the predominantly low ED of the cross polarization reference as compared to the high ED of the spatial references along the route (see Fig. 6) enables the cross polarization reference to have 12% higher capacity at the 50% outage level (see Fig. 7). In fact, the peak improvement with the cross polarization reference along the 600 m route is as high as 21%. The spatial reference has similar capacity performance as the prototypes since, despite its high channel gain, it has high ED.

The average performances at the local sections along the route give an indication of the potential benefit of reconfiguring the antenna system to maximize capacity. If instantaneous switching between TX-RX configurations with different terminal prototypes at RX is applied to maximize capacity at each point of the route (i.e., "Max capacity" in Fig. 7), the improvement in 50% outage capacity is 6%, relative to

the worst performing configuration (i.e., prototype B). On the other hand, if the worst configuration for the few chosen local sections (i.e., prototype C) is used as the reference, the improvement is in fact lower, at 4%. These improvements are consistent to that obtained from dual variable-length reconfigurable dipoles that are simulated in an outdoor environment in [9]. There, an 8% gain, at SNR = 20 dB, is achieved as compared to a fixed antenna configuration.

Despite the modest statistical improvements obtained over the entire route, the gains are much higher locally. Furthermore, the peak improvements also suggest that higher capacity gains may be achieved, if the switching is performed faster (i.e., for less than 10 m). It should be emphasized that the antenna topologies in this study are not optimized for demonstrating the potential of reconfigurability (e.g., the antenna patterns across different prototypes are not completely orthogonal). Notwithstanding, they highlight the importance of different antenna radiation characteristics for better antenna-channel interaction, which improves capacity.

B. Interference-Limited (IL) Scenario

In the previous section, we assumed that the 2×2 MIMO link is established between the MS and the BS sector (of cross polarized antenna) with the highest channel gain at each measurement point. Here, we consider the two remaining BS sectors (each with a cross-polarized antenna) as interference sources in the capacity evaluation.

In general, the introduction of interference results in similar degradation in capacity for all the prototype cases, relative to the NL case. Thus, overall, there are no significant capacity differences between the prototypes, as shown in Fig. 7. However, since the characteristics of the interference vary along the route, its impact on capacity differs locally. Over the 600 m route, it is the interferences from Sectors 1 and 2 that have the most influence, since the interference power from Sector 3 is at or below the noise floor, due to its coverage area (see Fig. 1). Thus, the Sector 3 interference is perceived by the established 2×2 link as white noise over the entire 600 m.

The signal-to-interference ratio (SIR) determines the severity of the capacity degradation. In LOS, at 260 m, the degradation in the 10 m section is between 36% and 40% for all three configurations, due to SIR levels in the range of 16-20 dB. At 430 m (NLOS), the SIRs are lower, at 12-14 dB, and consequently the degradation is even higher (~59%). Finally at 460 m (NLOS), the SIRs are within the range 7-9 dB and the degradation is up to 73%.

Whereas for all three prototype configurations at all three local sections (i.e., centered at 260 m, 430 m and 460 m) the interference channels have similar ED (ES ~0.6), the ED performances of the desired channels are different, as discussed in Section IV-A. The degradation from the NL to the IL scenario is mainly dependent on the SIR, but there are indications that ED of the desired channel influences the ability of the desired channel to suppress interference. However, this has to be further investigated.

The local performances in the IL scenario also indicate the potential of antenna reconfigurability in maximizing capacity. For example, at 260 m, as shown in Table II, prototype B has 11% higher capacity than the worse performing prototype (i.e., prototype A). Moreover, the peak improvements are up to 28%. If prototype A is also the "fixed configuration" for the two other 10 m local sections, then at 460 m, the average capacity from using the best case (i.e., prototype B) is 20% higher than the fixed configuration. At 430 m, however, the average capacities of prototypes B and C are below that of the fixed configuration, and thus no gain is achieved. Overall, the capacity gain at 50% outage is 8%, relative to the fixed configuration of prototype B, if instantaneous switching for maximum capacity is applied along the route (see "Max capacity" in Fig. 7). If the fixed configuration is prototype A or C, the 50% outage capacity gain is merely 3%.

V. CONCLUSIONS

Three dual-antenna topologies, each in a simplified prototype of size and shape typical of today's smart phones, are evaluated in extensive 2×2 MIMO channel measurements at 2.65 GHz. The measurements took place in a three-sector base station (BS) site in an urban macrocellular environment. The evaluation is performed for both NL and IL scenarios.

Our results show that, overall, the three dual-antenna systems at the RX end perform similarly along a 600 m route. However, the average capacities over 10 m route sections can differ by up to 16% and 20% between the best and worst (fixed) antenna configurations in the NL and IL scenarios, respectively. Moreover, if we compare the average capacity performance over 1.1 m sections, peak gains along the route are up to 18% for the NL scenario and 28% for the IL scenario.

Locally, the three configurations enable different synergies between channel gain and ED due to their different radiation performances (efficiencies and angular/polarization patterns). Thus, different capacities are obtained. The importance of ED is highlighted in the cases of the evaluated spatial and cross polarization reference configurations. In particular, the spatial reference with significantly higher channel gain than the evaluated prototypes has similar capacity to those of the prototypes, due to its high ED.

Choosing one of the three antenna topologies over the others for implementation in MIMO terminals does not provide significant gain in capacity in FS, when the 50% outage capacity over the 600 m route is considered. However, the differences in local performances indicate some potential benefit of antenna reconfigurability to maximize capacity. If switching between configurations for maximum capacity is applied along the entire 600 m route, 3-8% gain can be expected at 50% outage, depending on the choice of the reference (fixed) antenna configuration. Locally, this gain is higher and dependent on how fast the switching is performed.
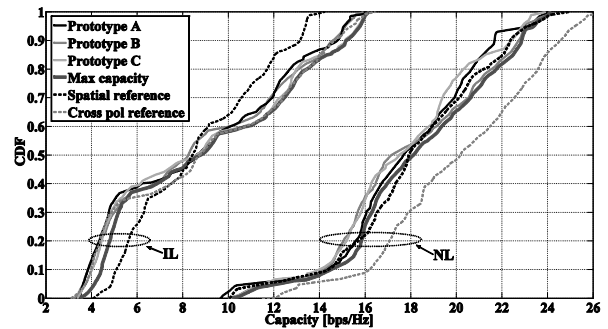
ACKNOWLEDGMENT

Fig. 7 CDFs of capacity performances along the 600 m route in NL and IL scenarios for the TX-RX configurations with terminal prototypes and references at the RX.

TABLE II
AVERAGE CAPACITY FOR LOCAL ROUTE SECTIONS

Route section (10 m)	Antenna configuration at RX	Average capacity [bps/Hz] NL scenario	Average capacity [bps/Hz] IL scenario
@ 260 m (LOS)	A	20.0	12.2
	B	22.6	13.6
	C	19.4	12.4
@ 430 m (NLOS)	A	20.3	8.4
	B	18.6	7.6
	C	18.7	7.7
@ 460 m (NLOS)	A	20.9	6.0
	B	22.7	7.2
	C	20.2	5.5

REFERENCES

[1] D. W. Browne, M. Manteghi, M. P. Fitz, and Y. Rahmat-Samii, "Experiments with compact antenna arrays for MIMO radio communications," *IEEE Trans. Antennas Propagat.*, vol. 54, no. 11, pp. 3239–3250, Nov. 2006.

[2] Y. Selén and H. Asplund, "3G LTE simulations using measured MIMO channels", *in Proc. IEEE Global Telecommun. Conf.,* New Orleans, LA, Nov. 30-Dec. 4, 2008, pp. 1-5.

[3] M. Hunukumbure and M. Beach, "MIMO channel measurements and analysis with prototype user devices in a 2GHz urban cell," *in Proc. IEEE 17th Int. Symp. on Personal, Indoor and Mobile Radio Commun. (PIMRC)*, Helsinki, Finland, 2006, Sep. 11-14, 2006.

[4] J. Salo, P. Suvikunnas, H. M. El-Sallabi, and P. Vainikainen, "Some results on MIMO mutual information: the high SNR case," *in Proc. IEEE Global Telecommun. Conf.,* Dallas, TX, Nov. 29-Dec. 3, 2004, pp. 943- 947.

[5] J. Salo, P. Suvikunnas, H. M. El-Sallabi, and P. Vainikainen, "Ellipticity statistic as a measure of MIMO multipath richness," *Electron. Lett.*, vol. 42, no. 3, pp. 45-46, Feb. 2006.

[6] G. J. Foschini and M. J. Gans, "On limits of wireless communications in a fading environment when using multiple antennas*," Wireless Personal Commun.*, vol. 6, pp. 311-335, 1998.

[7] Y. Song and S. D. Blostein, "MIMO channel capacity in co-channel interference," in *Proc. 21st Biennial Symp. Commun.*, Kingston, Canada, Jan. 2002, pp. 220–224.

[8] P. Suvikunnas, J. Salo, L. Vuokko, J. Kivinen, K. Sulonen, and P. Vainikainen, "Comparison of MIMO antenna configurations: methods and experimental results," *IEEE Trans. Veh. Technol.,* vol. 57, no. 2, Mar. 2008.

[9] D. Piazza, N. J. Kirsch, R. W. Heath, A. Forenza, and K. R. Dandekar, "Design and evaluation of a reconfigurable antenna array for MIMO systems," *IEEE Trans. Antennas Propagat.*, vol. 56, no. 3, pp. 869-881, Mar. 2008.